REVISTA DE LA
ASOCIACIÓN GEOLÓGICA ARGENTINA
www.geologica.org.ar

Volumen 81 (1)
MINERALOGÍA, PETROGÉNESIS Y METALOGENIA VINCULADA A MINERALES DE MENA METALÍFEROS Y NO METALÍFEROS DE ARGENTINA

Abril 2024

The association of niobian rutile, columbite-group minerals and uranium-rich pyrochlore in the Rancul granitic pegmatite, San Luis, Argentina

Miguel Ángel GALLISKI[1*], María Florencia MÁRQUEZ-ZAVALÍA[1,2], María Belén ROQUET[3], Milan NOVÁK[4] and Radek ŠKODA[4]

[1] IANIGLA, CCT CONICET Mendoza. Mendoza, Argentina.

[2] Mineralogía y Petrología, FAD, Universidad Nacional de Cuyo, Centro Universitario. Mendoza, Argentina.

[3] Departamento de Geología, Universidad Nacional de San Luis, San Luis, Argentina.

[4] Department of Geological Sciences, Masaryk University, Kotlářská 2, 611 37 BRNO, Czech Republic.

Emails: galliski@mendoza-conicet.gov.ar; mzavalia@mendoza-conicet.gov.ar; belenroquet@gmail.com; milangeo@seznam.cz; rskoda@sci.muni.cz

Editor: María Florencia Gargiulo

Recibido: 29 de Junio de 2023
Aceptado: 17 de octubre de 2023

ABSTRACT

We describe the mineralogy of the association of accessory niobian rutile, columbite-group minerals and an uranium-rich pyrochlore-like phase that occur in the Rancul property (32º38'50" S, 65º40'46" W), an NYF intragranitic pegmatite of the Potrerillos group, San Luis, Argentina. Other accessory and secondary minerals include biotite, muscovite, beryl, schorl, apatite, ilmenite, pyrite, bismuthinite, clinobisvanite, hematite, and goethite. Niobian rutile occurs as rare cm-sized prismatic crystals in the core-margin assemblage usually enclosed in quartz or albite. It has Ti# [Ti/(Ti+Nb+Ta)] variable between 0.81 and 0.92 and contents of TiO_2 between 63.46 and 80.21 wt.%, Nb_2O_5 ≤ 21.66 wt.%, most of the iron as Fe_2O_3, low UO_2 and Sc_2O_3. The contents (wt.%) of Ta_2O_5 are variable, reaching up to 7.86, of WO_3 ≤ 1.46, of SnO_2 ≤ 1.12, of Sc_2O_3 ≤ 0.37 and of ZrO_2 ≤ 0.15. The structure is that of monorutile (space group $P4_2/mnm$) and the cell parameters are a = 4.622 (2) Å; c = 2.983 (2) Å; V = 63.73 (5) Å^3. The rutile has inclusions of a columbite-group mineral, likely disordered columbite, and a U-rich pyrochlore-group mineral with up to 53.66 wt.% of UO_2 accompanied by niobian rutile with higher Ti# and lower content of trace elements. They are not exsolution products and were produced along subparallel cracks possibly by Ca,Mn,U-rich aqueous fluids that reworked the primary niobian rutile leaching the trace elements and crystallizing the new mineral phases.

Keywords: Niobian-rich minerals, NYF rare-element pegmatite.

RESUMEN

La asociación de rutilo niobífero, minerales del grupo de la columbita y pirocloro rico en uranio de la pegmatita granítica Rancul, San Luis, Argentina.

Describimos la asociación de minerales accesorios integrada por rutilo niobífero, un mineral del grupo de la columbita y pirocloro rico en uranio que ocurre en Rancul (32º38'50" S, 65º40'46" O), una pegmatita intragranítica de familia petrogenética NYF del grupo Potrerillos, San Luis, Argentina. Otros minerales accesorios y secundarios incluyen biotita, muscovita, berilo, chorlo, apatita, ilmenita, pirita, bismutinita, clinobisvanita, hematita y "limonita". El rutilo niobífero se presenta como escasos cristales prismáticos centimétricos en la asociación de borde de núcleo, generalmente incluido en cuarzo o albita. Posee Ti# [Ti/(Ti+Nb+Ta)] variable entre 0.81-0.92 y contenidos de TiO_2 entre 63.86 y 80.21 % en peso, Nb_2O_5 ≤ 21.66 % en peso, la mayor parte del hierro como Fe_2O_3, bajo UO_2 y Sc_2O_3. Los contenidos (% en peso) de Ta_2O_5 son variables llegando hasta 7.86, WO_3 ≤ 1.46, SnO_2 ≤ 1.12, Sc_2O_3 ≤ 0.37 y ZrO_2 ≤ 0.15. La estructura es la del monorutilo ($P4_2/mnm$) y los parámetros de celda son a = 4.622(2) Å; c = 2.983(2) Å; V = 63.73 (5) Å^3. El rutilo niobífero tiene inclusiones de un mineral del grupo de la columbita, probablemente columbita desordenada, y un mineral del grupo del pirocloro rico en U con hasta un 53.66 % en peso de UO_2 acompañado por rutilo rico en niobio con mayor Ti# y menor contenido de elementos traza. Estos minerales no son productos de exsolución y fueron producidos a lo largo de fracturas subparalelas posible-

mente por fluidos acuosos ricos en Ca-Mn-U que retrabajaron el rutilo niobífero primario lixiviando los elementos traza y cristalizando las nuevas fases minerales.

Palabras clave: Minerales ricos en niobio, pegmatita de elementos raros NYF.

INTRODUCTION

The occurrence of niobian rutile (formerly ilmenorutile, now discredited) as accessory mineral in rare-element granitic pegmatites has been noted long ago and studied in many opportunities (e.g., Černý et al. 1964, Černý et al. 2007 and references therein). However, its association with different related mineral phases, and its subsolidus transformations processes are always a reason of interest in the study of pegmatites. In LCT (Li-Cs-Ta; in the sense of Černý 1991) rare-element pegmatites of Argentina, tantalian rutile occurs as a subsolidus phase replacing tantalite-(Mn) in some beryl-type pegmatites such as Nancy, San Luis (Galliski et al. 2019) or La Calandria, Córdoba (Galliski et al. 2016), but niobian rutile is not a common phase. It was described in: (1) the alluvial sediments of the northern border of Las Chacras-Potrerillos batholith (Lira et al. 1987), (2) from a greissen mineralization in a paragenesis of cassiterite, wolframite, fluorite, K-feldspar, tourmaline, muscovite, pyrite and arsenopyrite (Fernández et al. 2005), (3) in aplite-pegmatites and pegmatitic pods related with the A-type El Portezuelo granite (Colombo 2008) and (4) a little-transported pebble found in an environment of amphibolite-grade metamorphic rocks intruded by pegmatites and hydrothermal veins in Copalayo gulch, Centenario ridge, Puna, Salta (Lira et al. 2018).

In this paper we describe an association of primary niobian rutile in a NYF-type rare-element granitic pegmatite from the intragranitic Potrerillos group, the associated secondary minerals and the probable origin of them caused by subsolidus reworking.

GEOLOGICAL SETTING OF THE RANCUL PEGMATITE

The Rancul pegmatite is located at 32º38´50” S and 65º40´46” W, approximately at 1150 m above sea level in the Libertador General San Martín department of the San Luis province, Argentina. The detailed geology of the pegmatite was described by Roquet (2010), a synopsis of the Potrerillos group of pegmatites by Roquet et al. (2011), and the main geological features of the pegmatites and the host granite by Lira et al. (2012). Niobian rutile was identified in the Rancul and Potrerillos 2 pegmatites. The description of the Rancul pegmatite is based on Roquet (2010). The Rancul property consists of three main bodies of irregularly shaped pegmatites (Fig. 1), enclosed in a medium-grained Kfs-Qz-Pl-Ms-Bt monzogranite belonging to the muscovite-bearing red granite of the Potrerillos pluton (Lira et al. 2012). The pegmatites have an irregular zonation formed by border-wall, intermediate and core zones, plus several replacement units. The granitic host-rock passes transitionally by increased grain size to the border and wall zones of the pegmatite that show similar mineralogy but different grain-size.

The intermediate zone made by Kfs-Qz±Bt±Ms shows very coarse grain size with euhedral to subhedral crystals of highly ordered microcline included in grey to white massive quartz. The pegmatite shows replacement units of different types: 1) biotite-bearing irregular pods formed by black biotite crystals up to 30 cm in size, although generally smaller; 2) tourmaline-bearing units formed by massive to fibroradiating crystals of schorl; 3) areas rich in fine-grained muscovite (2M_1 polytype), commonly developed on faces or fractures in microcline, and 4) minor fine-grained albite accumulations between the intermediate and core zones and usually associated with accessory minerals. The core zone is represented by massive milky to light grey quartz and less of 5 % vol. of schorl, fluorapatite, pyrite and ilmenite. Light green beryl, niobian rutile, and dark red porous hematite, altered bismuth minerals and goethite are associated with Qz±Kfs±Ab in dump samples that probably come from the core margin association.

MATERIALS AND METHODS

One polished thin section and two conventional polished sections, mounted in epoxy in 2.54 cm diameter discs, were prepared with selected samples. The samples were grinded and polished following the procedure of Craig and Vaughan (1994). The polished sections were studied under reflected light in air, prior to carbon coating, in a Leica DM2500P optical polarizing microscope, in order to describe them and to select suitable spots for electron-microprobe analyses.

The first batch of chemical analyses was obtained at the

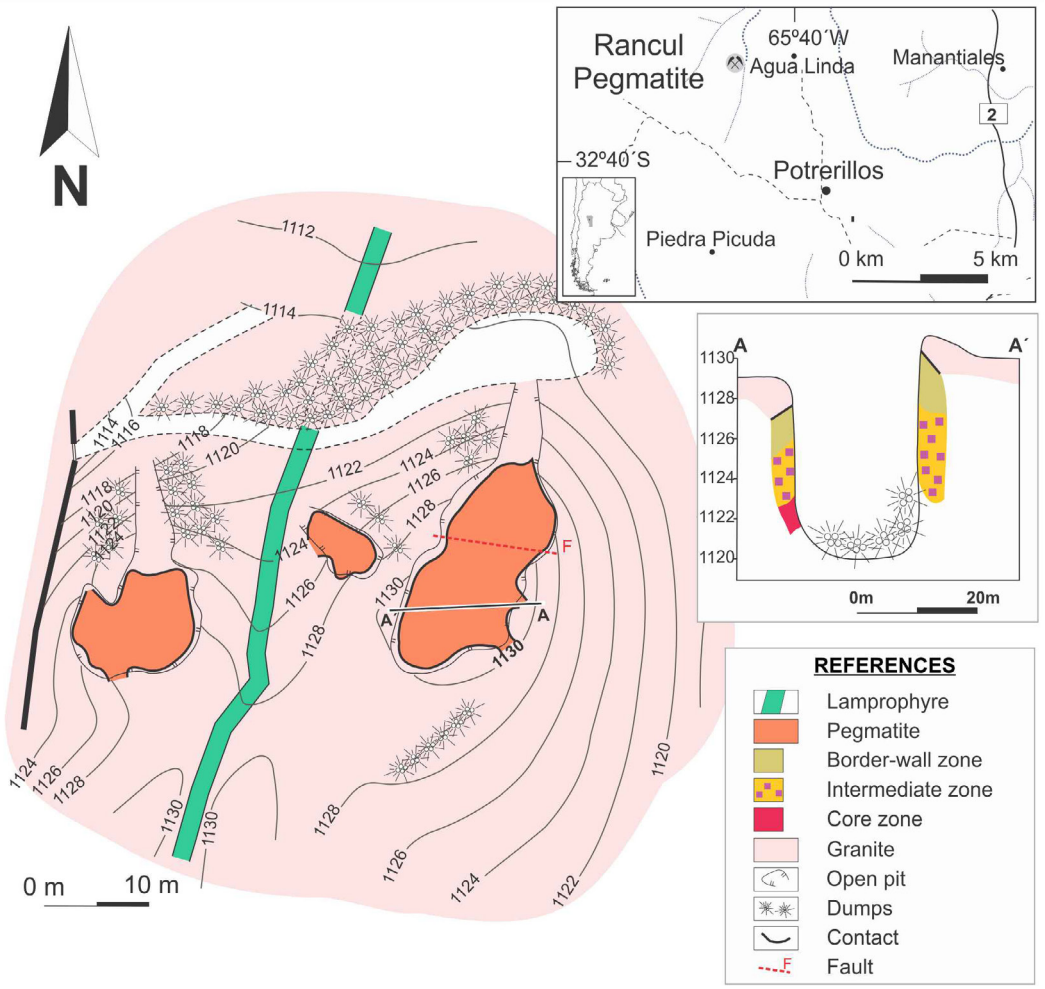

Figure 1. Location map of the Rancul pegmatite showing the main geological units of the area; inset shows A-A' profile with the zoning of the main body of the property.

Department of Geological Sciences, University of Manitoba, Winnipeg, Canada; they were performed with a CAMECA SX-100 electron microprobe, with an accelerating voltage of 15 kV, beam current of 20 nA, counting times of 20s for each element and 10s for each background position and a beam diameter of 2 μm. The standards (analytical lines selected -*K*α lines unless specified-; limits of detection in wt.%) are: microlite (Na; 0.04), $MnNb_2Ta_2O_9$ (TaM_α; 0.18), $CaNb_2O_6$ (Ca; 0.02), $FeNb_2O_6$ (Fe; 0.06), $MnNb_2O_6$ (NbL_α; 0.12), $MnNb_2O_6$ (Mn; 0.06), orthoclase (K; 0.03), rutile (Ti; 0.07), stibiotantalite (SbL_α; 0.09), SnO_2 (SnL_α; 0.10), $CaWO_4$ (WL_α; 0.36), mimetite (PbM_β; 0.40), $BiTaO_4$ (BiM_β; 0.13), UO_2 (UM_β; 0.24), diopside (Si; 0.02), $SrBaNb_4O_{12}$ (SrL_α; 0.10), pollucite (CsL_α; 0.06), $Ba_2NaNb_5O_{15}$ (BaL_α; 0.32), and ZrO_2 (ZrL_α; 0.06). The data were reduced using the PAP routine (Pouchou and Pichoir 1985).

Additionally, the minerals were analyzed in the wavelength-dispersion mode with a CAMECA SX-100 electron microprobe at the Laboratory of Electron Microscopy and Microanalysis, the joint facility of the Masaryk University and the Czech Geological Survey in Brno, Czech Republic. The following analytical conditions were applied: acceleration voltage 15 kV and beam current 20 nA; the beam diameter was 2 μm. The following standards were used (*K*α lines unless spec-

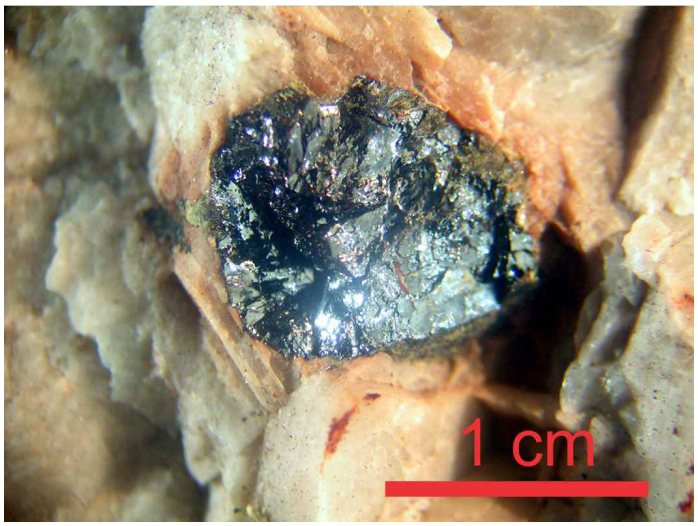

Figure 2. Photograph of one dark grey cm-sized prismatic crystal of niobian rutile with the [001] axis approximately normal to the surface of the sample, included in plagioclase in the core-margin association of the Rancul pegmatite. Note the oxidation halo around the crystal.

ified; limits of detection in wt.%): albite (Na; 0.04), $CaTh(PO_4)_2$ (ThM_α; 0.02), gahnite (Al, Zn; 0.02, 0.03), hematite (Fe; 0.05), lammerite (AsL_α; 0.07), sanidine (Si, K; 0.02), $MgAl_2O_4$ (Mg; 0.02), titanite (CaK_β; 0.08), YPO_4 (YL_α; 0.05), Mn_2SiO_4 (Mn; 0.04), vanadinite (PbM_β; 0.05), TiO_2 (Ti; 0.07), zircon (ZrL_α; 0.05), Nb (NbL_α; 0.06), $CrTa_2O_6$ (TaM_α; 0.08), $ScVO_4$ (Sc; 0.03), Sb (SbL_β; 0.18), Sn (SnL_α; 0.13), Bi (BiM_β; 0.14), W (WL_α; 0.10) and U (UM_β; 0.05).

Back-scattered electron (BSE) images were acquired to document the compositional variation of the individual phases and to show their textural relationships and the location of the analyses. The formulae and the Fe^{2+}/Fe^{3+} ratio were calculated according to stoichiometry and charge-balance considerations.

The X-ray powder diffraction pattern of the minerals were obtained using a Rigaku D-MAX III C diffractometer, with Cu anode (λ = 1.54184 Å). X-ray, at 30 Kv, 20 mA and were filtered with Ni. Patterns were measured with a speed of 0.3º (2Θ)/min at the Instituto de Investigaciones en Tecnología Química (INTEQUI), San Luis, Argentina. Cell-parameter refinements of the powder-diffraction data were carried out with the CELREF V3 program (Laugier and Bochu 2003).

RESULTS

Description of the minerals

Niobian rutile: The samples of niobian rutile show individ-

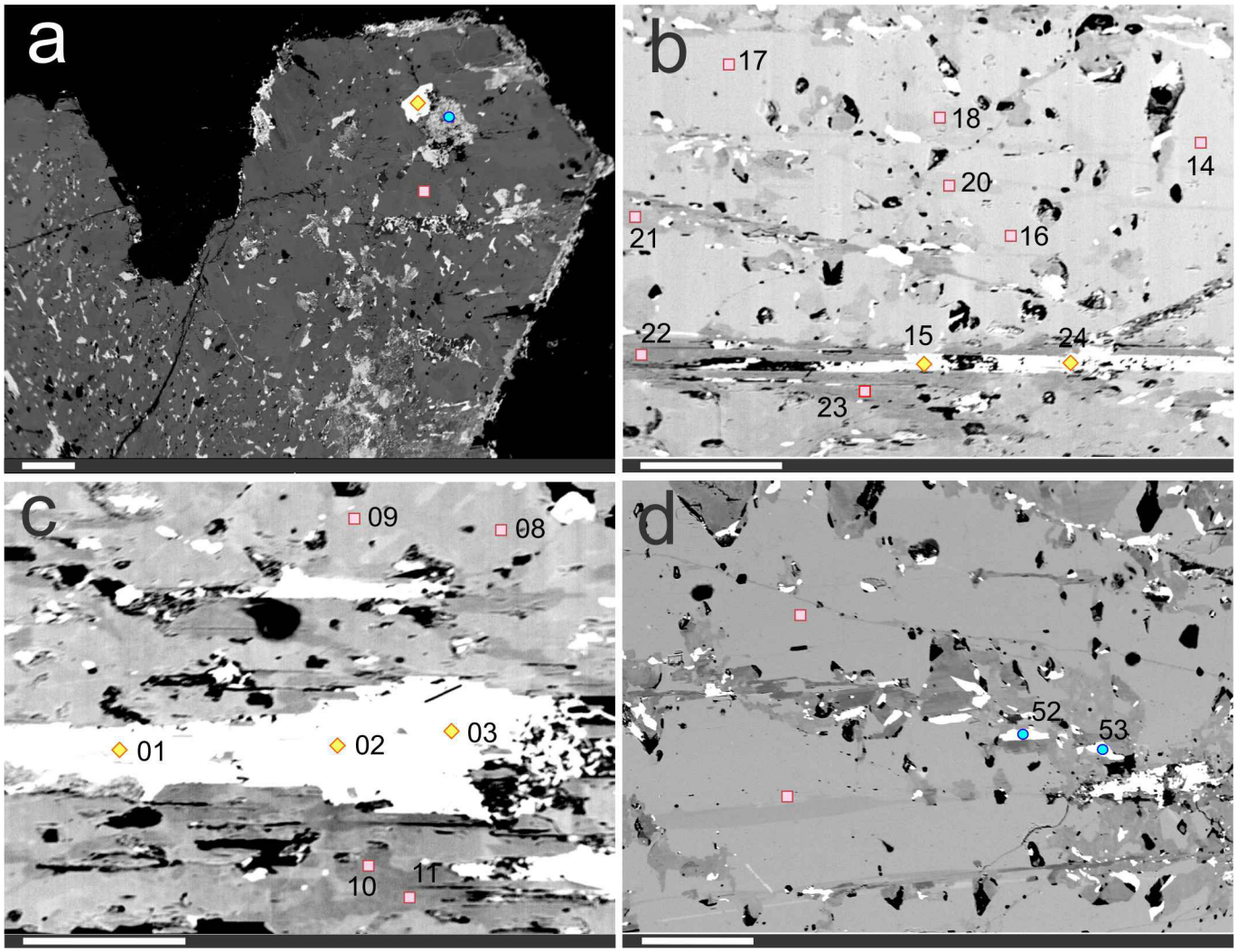

Figure 3. Back-scattered electron (BSE) images of the assemblage of oxides in the Rancul pegmatite: a) Euhedral crystal of niobian rutile showing the grains of the associated minerals. b) Niobian rutile (main phase) including darker areas along some shear planes showing elongated grains of niobian rutile with higher Ti#, and elongated and pale grey grains of pyrochlore-group minerals. c) Irregular elongated grain of pyrochlore-group minerals that includes some acicular crystals of rutile, all included in niobian rutile. d) Groundmass of niobian rutile including darker areas of the same phase with variable but higher Ti# and bright grains of columbite-group minerals. Scale bar in all images is 200 micrometers; square red symbols represent niobian rutile, blue circles columbite-group minerals, and yellow diamonds pyrochlore-group minerals; numbers indicate the point of chemical analyses.

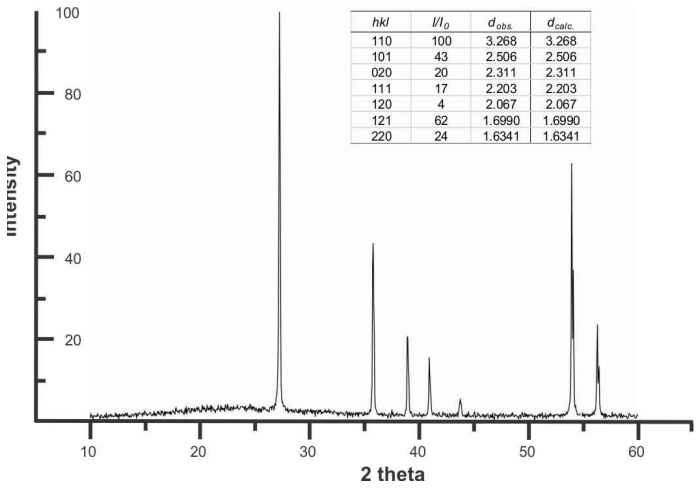

hkl	I/I_0	$d_{obs.}$	$d_{calc.}$
110	100	3.268	3.268
101	43	2.506	2.506
020	20	2.311	2.311
111	17	2.203	2.203
120	4	2.067	2.067
121	62	1.6990	1.6990
220	24	1.6341	1.6341

Figure 4. X-ray powder diffractogram of niobian rutile from Rancul pegmatite.

ual, sub- to euhedral prismatic crystals 1-2 cm (exceptionally up to 3 cm) long, enclosed in quartz or fine-grained albite (Fig. 2).

They are elongated and show parallel striations along [001], dark grey color with dark green streak and adamantine luster. In reflected light, niobian rutile is the main phase; it is grey with a slight pale blue tint, the pleochroism is not perceptible in air and the chemical variations, visible in BSE images, are not evident. The anisotropy is distinct, displaying different shades of grey and scarce internal reflections, from brown to yellowish or reddish brown. Niobian rutile hosts numerous inclusions. Under the optical microscope, elongated inclusions of polygranular muscovite and quartz occur along parallel discontinuities. Muscovite cleavage can be parallel or, less frequently, oblique to the cracks. The most common inclusions belong to columbite- and pyrochlore-group minerals. Niobian rutile also hosts frequent small (up to 5 μm), tabular inclusions, which are formed by two or three phases in different shades of grey and that under the crossed polarizers have abundant internal reflections (red, brown and orange); each of the phases is smaller than 1 μm, which prevents their identification. They possibly correspond to rutile + ilmenite-hematite exsolutions.

BSE images reveal two generations of niobian rutile; one is the main phase and others are located along the cracks. The different generations show different shades of grey in the BSE images (Fig. 3) reflecting the variable (Nb+Ta)/Ti) ratio (Table 1). The last generation commonly include brighter grains of columbite- and pyrochlore-group minerals. The X-ray diffraction diagram (Fig. 4) has an excellent coincidence with rutile from Věžná, Czech Republic (Černý et al. 1964). The cell parameters refined for the Argentine rutile give a = 4.622 (2) Å; c = 2.983 (2) Å; V = 63.73 (5) Å3. In the X-ray diagrams of niobian rutile there are not extra lines that could correspond to this or another phases.

Columbite-group minerals: Columbite-group minerals (CGM) occur as small (< 10 to 100 μm), sub- to anhedral inclusions, generally equidimensional to elongated, and mostly arranged following the general orientation of the cracks, but not along them. Under reflected light their colour is medium grey with a brownish hue, and they have slight pleochroism, from light to medium grey with a brown tint. They are strongly

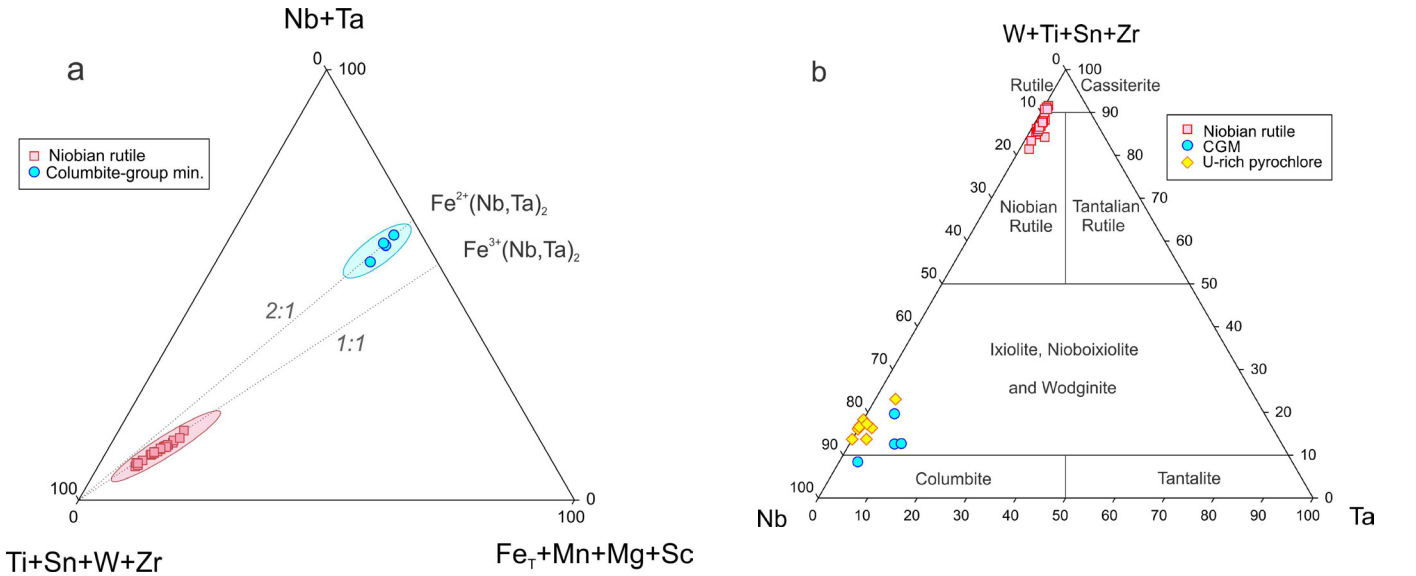

Figure 5. a) Ternary (FeT+Mn+Mg+Sc) - (Nb+Ta) - (Ti+Sn+W+Zr) diagram (at.%) showing the analyzed niobian rutile grains and the columbite-group minerals. b) Compositions of the assemblage of oxide minerals from the Rancul pegmatite in the diagram Ta – W+Ti+Sn+Zr – Nb (at.%), modified from Beurlen et al. (2007), showing the analyzed minerals and the chemical variabilities.

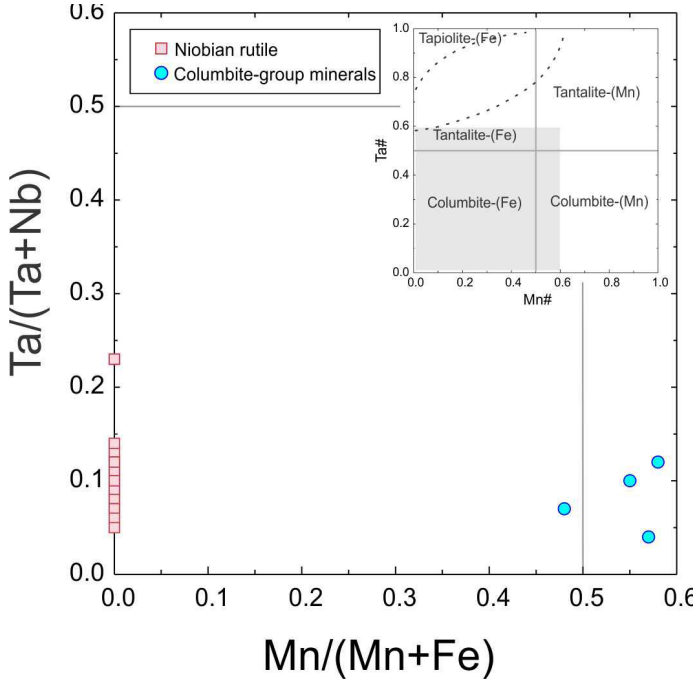

Figure 6. Columbite quadrilateral showing the compositions of niobian rutile and columbite-group minerals from the Rancul pegmatite. The gap between the fields corresponding to tapiolite-(Fe) and tantalite-(Fe) is taken from Černý et al. (1992a).

anisotropic, and no internal reflections were observed. The back-scattered images (Fig. 3d) show that there are subtle compositional differences between elongated crystals and anhedral patches. The size of the crystals and grains is too small for conventional X-ray diffraction methods.

Pyrochlore-group minerals: Grains of pyrochlore-group minerals occur along the subparallel cracks, associated with the last generation of niobian rutile (Fig. 3b, c); they are not intimately associated with CGM crystals. This isotropic mineral is medium grey and has abundant yellow to greenish-grey and brown internal reflections. Under crossed polarizers it can be seen that grains are not single crystals, as they appear when observed under parallel polarizers, but they are composed of a very fine microgranular material which together with the high UO_2 content suggests very low crystallinity.

Chemical composition of the minerals

Niobian rutile is compositionally heterogeneous as can be seen in BSE (Fig. 3). The lighter grey domains in BSE correspond to the dominant phase with a Ti# [= Ti/(Ti+Ta+Nb) apfu] ranging from 0.81 to 0.87, while the subordinate phases correspond to the intermediate grey color domains that have Ti# between 0.88 and 0.90 and the darker domains with #Ti above 0.90 (Table 1, Fig 3a-c).

The composition of the dominant primary phase shows, besides the lower Ti#, contents (wt.%) of TiO_2 between 63.46 and 68.48, Nb_2O_5 up to 21.66, and iron (mostly as Fe_2O_3, as calculated by stoichiometry) up to 10.14. The contents (wt.%)

Table 1. Representative chemical compositions of niobian rutile

	1st generation (Main phase)				2nd generation		
	46	47	48	49	10	11	45
WO_3	0.32	0.76	0.21	0.15	0.00	0.08	0.20
Nb_2O_5	21.66	17.92	17.40	15.67	12.91	11.60	11.26
Ta_2O_5	4.12	3.47	3.52	7.86	1.63	1.30	1.75
TiO_2	63.46	66.84	68.48	64.86	78.09	79.90	80.21
SnO_2	0.00	0.56	0.60	1.12	0.10	0.13	0.00
ThO_2	0.00	0.00	0.00	0.00	n.a.	n.a.	0.03
ZrO_2	0.11	0.09	0.06	0.00	0.01	0.04	0.08
SiO_2	0.03	0.00	0.02	0.02	0.04	0.03	0.04
Al_2O_3	0.07	0.11	0.09	0.10	n.a.	n.a.	0.05
Sc_2O_3	0.37	0.15	0.12	0.07	n.a.	n.a.	0.32
Bi_2O_3	0.00	0.00	0.00	0.00	0.00	0.00	0.20
Fe_2O_3	8.68	10.14	9.45	9.40	7.32	7.22	6.62
MgO	0.02	0.00	0.00	0.00	n.a.	n.a.	0.00
FeO	2.44	0.79	0.94	1.18	0.22	0.00	0.14
MnO	0.00	0.00	0.00	0.04	0.03	0.00	0.00
ZnO	0.00	0.00	0.03	0.00	n.a.	n.a.	0.05
Na_2O	0.00	0.04	0.00	0.00	0.06	0.06	0.00
TOTAL	101.28	100.92	100.92	100.47	100.41	100.36	100.94
W^{6+}	0.003	0.006	0.002	0.001	0.000	0.001	0.002
Nb^{5+}	0.289	0.237	0.229	0.212	0.165	0.147	0.143
Ta^{5+}	0.033	0.028	0.028	0.064	0.013	0.010	0.014
Ti^{4+}	1.408	1.470	1.498	1.461	1.657	1.684	1.687
Sn^{4+}	0.000	0.007	0.007	0.014	0.001	0.002	0.000
Th^{4+}	0.000	0.000	0.000	0.000	0.000	0.000	0.000
Zr^{4+}	0.002	0.002	0.001	0.000	0.000	0.001	0.001
Si^{4+}	0.001	0.000	0.001	0.001	0.001	0.001	0.001
Al^{3+}	0.003	0.004	0.003	0.004	0.000	0.000	0.002
Sc^{3+}	0.010	0.004	0.003	0.002	0.000	0.000	0.008
Bi^{3+}	0.000	0.000	0.000	0.000	0.000	0.000	0.002
Fe^{3+}	0.193	0.223	0.207	0.212	0.156	0.153	0.139
Mg^{2+}	0.001	0.000	0.000	0.000	0.000	0.000	0.000
Fe^{2+}	0.060	0.019	0.023	0.030	0.005	0.000	0.003
Mn^{2+}	0.000	0.000	0.000	0.001	0.001	0.000	0.000
Zn^{2+}	0.000	0.000	0.001	0.000	0.000	0.000	0.001
Na+	0.000	0.003	0.000	0.000	0.004	0.004	0.000
CATSUM	2.000	2.000	2.000	2.000	2.000	2.000	2.000
OXYGENS	4.000	4.000	4.000	4.000	4.000	4.000	4.000
Ta#	0.10	0.10	0.11	0.23	0.07	0.06	0.09
Mn#	0.00	0.00	0.00	0.00	0.00	0.00	0.00
Ti#	0.81	0.85	0.85	0.84	0.90	0.91	0.92

Formula contents on a basis of 2 cations and 4 anions.
U, Y, Sb, As, Ca, and Pb were below detection limits. n.a.: not analyzed.

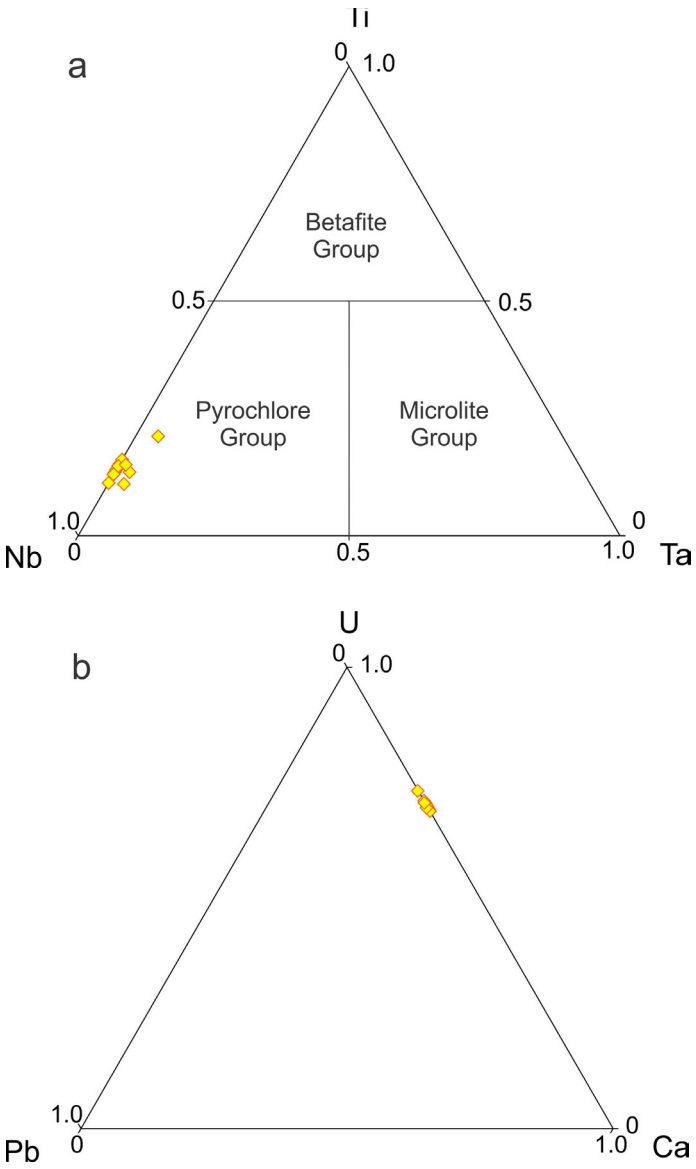

Figure 7. Composition of the pyrochlore-group minerals in a) the Ta-Ti-Nb ternary diagram to discriminate between the microlite, betafite and pyrochlore groups. b) The Ca-U-Pb ternary diagram.

of Ta_2O_5 are variable but reach up to 7.86, WO_3 up to 1.46, SnO_2 up to 1.12, Sc_2O_3 up to 0.37 and ZrO_2 up to 0.15, with negligible contents of CaO, MnO and Na_2O. The second generation of niobian rutile shows enrichment in TiO_2 and depletion in Nb_2O_5 and Ta_2O_5, with contents (in wt.%) of TiO_2 between 78.09 and 80.21, Nb_2O_5 between 11.26 and 12.91, Ta_2O_5 between 1.30 and 1.75, with most of the iron as Fe_2O_3 between 6.62 and 7.32. In the ternary (FeT+Mn+Mg+Sc) – (Nb+Ta) – (Ti+Sn+W+Zr) (Fig. 5a) diagram the compositions of the analysed minerals plot in the fields of niobian rutile and columbite-group minerals respectively. In the ternary Ta – (W+Ti+Sn+Zr) – Nb diagram modified from Beurlen et al. (2007) used to discriminate the different phases (Fig. 5b), most of the analyses plot in the field of ixiolite + nioboixiolite, owing to the relatively high contents of Ti, W, Sn, Zr, and Sc. However, since the chemical composition of ixiolite show Ta# > 0.5 (Černy and Ercit 1989) and that compositions with Nb-dominant are less frequent (Chukanov et al. 2023) the phase is probably a disordered columbite.

Table 2. Representative chemical compositions of columbite-group minerals

	52	53	15
WO_3	1.83	2.62	1.55
Nb_2O_5	60.40	60.83	67.16
Ta_2O_5	11.67	7.53	4.78
SiO_2	0.03	0.02	0.05
TiO_2	4.70	7.85	3.18
ZrO_2	0.45	0.45	0.24
SnO_2	0.38	1.06	0.08
UO_2	0.10	0.11	0.07
Sc_2O_3	1.03	1.03	0.77
Bi_2O_3	0.00	0.00	0.07
Fe_2O_3	0.82	1.45	0.73
FeO	7.59	8.27	7.59
MnO	10.17	8.90	10.78
CaO	0.00	0.00	0.13
TOTAL	99.16	100.13	97.17
W^{6+}	0.028	0.038	0.023
Nb^{5+}	1.594	1.549	1.768
Ta^{5+}	0.185	0.115	0.076
Si^{4+}	0.002	0.001	0.003
Ti^{4+}	0.206	0.333	0.139
Zr^{4+}	0.013	0.012	0.007
Sn^{4+}	0.009	0.024	0.002
$U4^{+}$	0.001	0.001	0.001
Sc^{3+}	0.052	0.051	0.039
Bi^{3+}	0.000	0.000	0.001
Fe^{3+}	0.036	0.061	0.032
Fe^{2+}	0.370	0.390	0.369
Mn^{2+}	0.503	0.425	0.532
Ca^{2+}	0.000	0.000	0.008
CATSUM	3.000	3.000	3.000
OXYGENS	6.000	6.000	6.000
Ta/(Ta+Nb)	0.10	0.07	0.04
Mn/(Mn+FeT)	0.55	0.49	0.57

Formula contents on a basis of 3 cations and 6 oxygens. Th, Pb, Y, Al, Sb, As, Mg, Zn and Na are below detection limits.

The chemical composition of the columbite-group minerals shows (Table 2) ranges in wt.% of Nb_2O_5 from 60.40 to 67.16, Ta_2O_5 4.78 to 11.67, MnO 8.90 to 10.78, FeO 8.24 to 9.58, WO_3 1.55 to 2.62, TiO_2 3.18 to 7.85, and maximum contents (in wt.%) of ZrO_2 0.45, SnO_2 1.06, UO_2 0.11, Sc_2O_3 1.03 and

Table 3. Representative chemical compositions of pyrochlore-group minerals

	W1	W2	W3	W4	W5	W13	W15	W24	B16	B17	B50	B51
WO_3	1.46	0.98	1.17	0.93	1.20	1.38	0.90	0.38	1.00	0.89	1.38	1.33
Nb_2O_5	19.38	22.22	20.32	22.12	20.51	23.38	22.14	22.50	21.73	19.54	22.09	22.50
Ta_2O_5	b.d.l.	b.d.l.	b.d.l.	b.d.l.	b.d.l.	b.d.l.	b.d.l.	b.d.l.	0.54	1.82	1.18	1.29
TiO_2	1.75	1.69	1.91	2.18	2.22	2.11	2.57	2.35	2.36	3.33	2.15	1.73
ZrO_2	0.18	0.15	0.17	0.14	0.18	0.15	0.13	0.20	0.10	0.12	0.09	0.07
SiO_2	0.69	0.76	0.72	0.86	0.74	0.81	0.75	0.81	1.74	1.60	0.72	0.76
Fe_2O_3	1.15	1.13	1.16	1.11	1.10	0.98	1.11	1.04	0.77	0.58	1.00	0.96
Al_2O_3	n.a.	n.a.	n.a.	n.a.	n.a.	n.a.	n.a.	n.a.	0.30	0.30	0.23	0.00
UO_2	51.54	52.32	51.35	53.46	51.16	52.30	52.84	52.26	51.29	52.69	53.66	53.43
Y_2O_3	n.a.	n.a.	n.a.	n.a.	n.a.	n.a.	n.a.	n.a.	0.26	0.24	0.11	0.14
Sc_2O_3	n.a.	n.a.	n.a.	n.a.	n.a.	n.a.	n.a.	n.a.	0.00	0.00	0.11	0.13
CaO	4.71	4.53	4.75	4.65	4.59	4.69	4.58	4.92	4.62	4.53	4.54	4.04
MnO	0.15	0.13	0.14	0.14	0.17	0.13	0.18	0.16	0.49	0.30	0.15	0.15
PbO	b.d.l.	b.d.l.	b.d.l.	b.d.l.	b.d.l.	b.d.l.	b.d.l.	b.d.l.	0.19	0.10	0.00	0.07
K_2O	0.13	0.13	0.11	0.17	0.19	0.22	0.11	0.16	0.00	0.00	0.00	0.00
Na_2O	b.d.l.	b.d.l.	b.d.l.	b.d.l.	b.d.l.	b.d.l.	b.d.l.	b.d.l.	0.12	0.13	0.00	0.15
F	n.a.	n.a.	n.a.	n.a.	n.a.	n.a.	n.a.	n.a.	0.00	0.00	0.00	0.00
H_2O *	0.91	0.99	0.94	1.02	0.97	1.06	1.04	1.03	1.10	1.09	1.05	1.03
O=F	0.00	0.00	0.00	0.00	0.00	0.00	0.00	0.00	0.00	0.00	0.00	0.00
TOTAL	82.05	85.03	82.74	86.78	83.03	87.21	86.35	85.81	86.61	87.26	88.46	87.78
U^{4+}	1.896	1.757	1.813	1.744	1.764	1.647	1.701	1.694	1.550	1.616	1.697	1.737
Y^{3+}	0.000	0.000	0.000	0.000	0.000	0.000	0.000	0.000	0.019	0.018	0.008	0.011
Sc^{3+}	0.000	0.000	0.000	0.000	0.000	0.000	0.000	0.000	0.000	0.000	0.014	0.017
Ca^{2+}	0.834	0.732	0.808	0.730	0.762	0.711	0.710	0.768	0.672	0.669	0.691	0.633
Mn^{2+}	0.021	0.017	0.019	0.017	0.022	0.016	0.022	0.020	0.056	0.035	0.018	0.019
Pb^{2+}	0.000	0.000	0.000	0.000	0.000	0.000	0.000	0.000	0.007	0.004	0.000	0.003
Na+	0.000	0.000	0.000	0.000	0.000	0.000	0.000	0.000	0.032	0.035	0.000	0.043
Σ A site	2.751	2.506	2.640	2.491	2.548	2.374	2.433	2.482	2.336	2.377	2.428	2.463
W^{6+}	0.063	0.038	0.048	0.035	0.048	0.051	0.034	0.014	0.035	0.032	0.051	0.050
Nb^{5+}	1.448	1.516	1.458	1.466	1.437	1.496	1.448	1.482	1.334	1.217	1.420	1.487
Ta^{5+}	0.000	0.000	0.000	0.000	0.000	0.000	0.000	0.000	0.020	0.068	0.046	0.051
Ti^{4+}	0.218	0.192	0.228	0.240	0.259	0.225	0.280	0.258	0.241	0.345	0.230	0.190
Zr^{4+}	0.015	0.011	0.013	0.010	0.014	0.010	0.009	0.014	0.007	0.008	0.006	0.005
Si^{4+}	0.114	0.115	0.114	0.126	0.115	0.115	0.109	0.118	0.236	0.220	0.102	0.111
Fe^{3+}	0.143	0.128	0.139	0.122	0.128	0.104	0.121	0.114	0.079	0.060	0.107	0.106
Al^{3+}	0.000	0.000	0.000	0.000	0.000	0.000	0.000	0.000	0.048	0.049	0.039	0.000
Σ B site	2.001	2.000	2.000	1.999	2.001	2.001	2.001	2.000	2.000	1.999	2.001	2.000
K^+	0.027	0.025	0.022	0.032	0.038	0.040	0.020	0.030	0.000	0.000	0.000	0.000
F^-	0.000	0.000	0.000	0.000	0.000	0.000	0.000	0.000	0.000	0.000	0.000	0.000
H^+	0.973	0.975	0.978	0.968	0.962	0.960	0.980	0.970	1.000	1.000	1.000	1.000
O^{2-}	9.875	9.507	9.672	9.458	9.533	9.286	9.341	9.389	9.028	9.103	9.348	9.458
CATSUM	4.778	4.531	4.662	4.523	4.586	4.413	4.453	4.512	4.336	4.376	4.429	4.461
AN SUM	9.875	9.507	9.672	9.458	9.533	9.286	9.341	9.389	9.028	9.103	9.348	9.458

* Determined by stoichiometry. H_2O calculated assuming 1(OH-, F-).

Formula contents o a basis of 2 B-site cations. Bi, Sr, are below detection limit (b.d.l.). n.a.: not analyzed.

low contents of MgO (up to 0.13). Those chemical compositions, plotted in the columbite-group minerals diagram (Fig. 6), are predominantly included in the field of columbite-(Mn) with one grain corresponding to columbite-(Fe).

The chemical composition of the pyrochlore-like mineral (Table 3) shows analyses with UO_3 up to 53.66 wt.%, Nb_2O_5 up to 23.38 wt.% and CaO up to 4.92 wt.%, with low total contents ranging from 82.05 to 88.46 wt.%. With this chemical composition it is reasonable to assign the phase to the pyrochlore supergroup minerals which have a general formula $A_{2-m}B2X_{6-w}Y_{1-n}$, where A = Na, Ca, Ag, Mn, Sr, Ba, Fe^{2+}, Pb^{2+}, Sb^{3+}, Bi^{3+}, Y, Ce (and other REE), Sc, U, Th, vacancy, H_2O. B = Ta, Nb, Ti, Sb^{5+}, W, V^{5+}, Sn^{4+}, Zr, Hf, Fe^{3+}, Mg, Al, Si. X = O, or minor OH and F. Y = OH, F, O, H_2O, K, Cs, Rb. The letters m, w, and n represent parameters that indicate incomplete occupancy of the A, X and Y sites, respectively. Calculation of the formula on a basis of B = 2 following Atencio et al. (2010) and Christy and Atencio (2013) shows that Nb is dominant in the B site and U in the A site (Table 3).

In the triangular classification diagram (Fig. 7a) the analyses plot in the Nb-dominant domain corresponding to the pyrochlore group. In the Ca-U-Pb triangular diagram (Fig. 7b) the analyses plot in the U-rich field. According to the assumed occupancy of the A site, these analyses correspond to a uranium dominant pyrochlore species that, although it has not been formally described (Atencio et al. 2010), is known from previous classification systems (Hogarth 1977, Hogarth and Horne 1989). Besides, it is quite possible that OH^- is the anion dominant in the Y-site since F is below the detection limit and no major amounts of alkalies suitable for this position (K, Cs, Rb) were detected. The significantly greater than 2.00 total of A-site cations is due to the high U content, expressed as UO_2, which in turn increases the O^{2-} content in the X-site to maintain charge balance (Zaitsev et al. 2021). That fact and the low totals from the analyses of this metamict mineral could be the consequence of the combination of several factors: 1) a gain of U in metamict domains, (e.g., similar gain of extraneous elements is well documented in metamict zircons (Geisler et al. 2007), in a form of sorption or in a presence of U-rich (e.g. uraninite) clusters, 2) low totals could indicate that the mineral had to release some elements and obtain H_2O, and although the B-site elements are considered relatively immobile with respect to those at site A, under certain conditions some elements could be leached out and replaced by OH groups, 3) the presence of microporosity, typical for metamict phases also decreases the analytical totals (Nasdala et al. 2009). This scenario could be supported by the null content of F and the low content of Na. The problems for solving the crystal structure of this material (small grain size, and most probably a highly metamict state produced by structural damage due to alpha-recoil) prevent a more detailed characterization of this phase with pyrochlore-like composition.

DISCUSSION

Comparison of niobian rutile compositions from NYF and LCT pegmatites

Niobian rutile is a typical primary and secondary Nb-Ta-Ti-oxide mineral in a variety of granitic pegmatites including LCT (e.g., Černý et al. 2000, 2007, Okrusch et al. 2003, Klementová and Rieder 2004, Beurlen et al. 2007, Novák et al. 2008) and NYF families (e.g. Černý et al. 1999, 2000). It mostly occurs in Li-poor pegmatites of beryl-columbite subtype and only scarcely in Li-rich spodumene-subtype pegmatites (e.g., Klementová and Rieder 2004, Beurlen et al. 2007). The chemical composition of niobian rutile from the Rancul NYF pegmatite differs significantly from niobian rutile in LCT pegmatites in the very high Fe^{3+} content (≤ 0.45 apfu). In this sense, rutile from other NYF pegmatites also have very high Fe^{3+}, some examples are Håverstad, Iveland, Norway (Fe^{3+} ≤ 0.52 apfu; Černý et al. 2000) and McGuire, Colorado, USA (Fe^{3+} ≤ 0.35 apfu; Černý et al. 1999). In contrast, the concentrations of some minor to trace elements (Sn, Sc, Zr) are similar in niobian rutile from NYF and LCT pegmatites (see the citations above); only W is typically higher in LCT pegmatites. The Ta/(Ta+Nb) ratios and ∑Nb+Ta vary significantly in niobian rutile but do not show any relation to either LCT or NYF families; however, tantalian rutile is typical solely for LCT pegmatites (Beurlen et al. 2007). The very high Mn/(Mn+Fe) ratio (up to ≤ 0.58, Fig. 6) of columbite-(Mn) associated with niobian rutile is unusual compared to other NYF and most LCT pegmatites except for the Capoeira and Quintos pegmatites, Borborema pegmatite district, Brazil (Beurlen et al. 2007), where columbite-(Mn) has Mn/(Mn+Fe) ratios up to 0.60 and 0.87, respectively. The high Mn# could be explained if the fluids have high oxygen fugacity producing that most of the Fe is present as Fe^{3+} and there is less Fe^{2+} available for entering in the columbite-(Mn) structure where it is preferred.

Textural relations and stages of crystallization of the Nb-Ta-Ti-oxide minerals

The identity of niobian rutile was confirmed by structural (X-ray diffraction, Fig. 4) and chemical methods. Its chemistry is changing from the primary grains, the volumetrically dominant phase, to the late generation grains with higher Ti# and lower minor and trace elements contents located along

the subparallel cracks and associated with later phases. The grains with chemical compositions of the columbite-group minerals [columbite-(Mn) > columbite-(Fe)] (Fig. 6) show, related to the niobian rutile, increasing contents of W, Ta, Zr and Sc (Tables 1 and 2). It is possible that the two styles of columbite occurrences, as anhedral irregular masses and as minor, subhedral crystals formed along some of the rutile cracks, are related to in situ formation (Fig. 3a) and to local transport in the adjacencies of physical discontinuities of the hosting niobian rutile (Fig. 3d), respectively.

It is supposed that niobian rutile, with significant contents of minor and trace elements, mainly Fe^{2+}, Fe^{3+}, W, Ta, Sn, Zr, Sc, plus lower contents of U, Zn, Ca and Na, all elements that by different substitution mechanism enter in the rutile structure (see e.g., Černý and Ercit 1989 or Rabbia and Hernández 2012), crystallized primarily when the pegmatitic melt, enriched in incompatible HFSE elements, reached a hydrous fluid phase possibly during formation of the core-margin mineral association. The evidence that the main niobian rutile phase is primary is not definitive but there are several signs. One is that the formation of the main niobian rutile phase is not showing replacement textures, as occurs with the second generation of niobian rutile. Another milder fact is that the quartz and muscovite crystals included in the niobian rutile follow the striations of the host phase. The third evidence is that being the primary niobian rutile the richest in trace elements, after the breakdown of the host, these trace elements recombine to give the associated minerals: niobian rutile with higher Ti# and lower contents of trace elements, and likely disordered columbite and uranium-rich pyrochlore-like phase. This interpretation was used to explain other occurrences of niobian rutile by Černý et al. (1981, 1999) and Černý and Chapman (2001). This subsolidus reworking of the niobian rutile possibly occurs by means of oxidizing aqueous solutions that released the cations from magmatic niobian rutile with subsequent recrystallization of secondary rutile with higher Ti# and disordered columbite. The source of U in the uranium-rich pyrochlore, as well as the Ca and eventually most of the Mn from the columbite-(Mn), could be derived from the usual last stage subsolidus process called “miniflood of Ca” by Martin and De Vito (2014). However, very high contents of U in secondary uranium-rich pyrochlore, as well as high Mn contents in the associated secondary columbite-(Mn), are unusual. They were very likely sourced by fluids exsolved from a residual melt as was documented in Ca-rich secondary Be-minerals from intragranitic NYF pegmatites of the Třebíč Pluton, Moldanubicum, Czech Republic (Zachař et al. 2020). Černý et al. (1992b) and Chládek et al. (2020, 2021) described from beryl-columbite pegmatites at Maršíkov, Silesicum, Czech Republic, multiphase alterations of primary columbite including several generations of secondary columbite and microlite-group minerals (variable in Ca, Na, U and F) with distinct sources of fluids. However, textural relations of secondary columbite and pyrochlore do not indicate multiphase processes. Some link between these fluids and the lamprophyre dike that closely cut across the granite is possible but improbably at this stage of the research.

CONCLUSIONS

The study of the accessory niobian rutile and its associated phases, (columbite-group minerals and uranium-rich pyrochlore), from the Rancul granitic pegmatite of the NYF petrogenetic family allows us to conclude that:

The niobian rutile formed as a primary mineral from a pegmatitic melt in the last stage of pegmatite solidification, structurally including as minor and trace elements: W, Sn, Th, Zr, Si, and Sc.

After magmatic crystallization, niobian rutile experienced subsolidus reworking yielding columbite-group minerals, likely disordered columbite-(Mn), a uranium-rich pyrochlore-group mineral, and secondary niobian rutile grains with increasing and variable Ti#.

The transformation was probably facilitated by an oxidizing Ca,Mn,U-rich aqueous fluid phase that locally hydrothermally reworked the primary niobian rutile along its subparallel fractures refining its chemical composition.

ACKNOWLEDGEMENTS

We are very glad to dedicate this paper as a tribute to the career of Milka K. de Brodtkorb, for her prominent achievements in the development of mineralogy in Argentina, especially in the study of ore minerals and its deposits. Grants from Consejo Nacional de Investigaciones Científicas y Técnicas (CONICET) to MAG and MFM-Z in several opportunities supported some of the field work and analytical results. The authors are very grateful to the Ministerio de Ciencia, Tecnología e Innovación Productiva de la República Argentina (MINCYT), Argentina and the Ministry of Education, Youth and Sports (MEYS), Czech Republic for the cooperation projects ARC/13/14 and 7AMB14AR006, which facilitated the execution of this research project. Early chemical analyses of the assemblage were obtained in the Department of Geological Sciences of the University of Manitoba thanks to the kind help of the late Dr. Petr Černý who was a dedicate researcher of

niobian rutile. The authors are grateful to Dr. F. Colombo for the careful revision of the manuscript, as well as to an anonymous reviewer and to Dr. F. Gargiulo for the editorial revision and improvement of the manuscript.

REFERENCES

Atencio, D., Andrade, M.B., Christy, A.G., Gieré, R. and Kartashov, P.M. 2010. The pyrochlore supergroup of minerals: nomenclature. The Canadian Mineralogist 48(3): 673-698.

Beurlen, H., Barreto, S.B., Silva, D., Wirth, R. and Olivier, P. 2007. Titanian ixiolite - niobian rutile intergrowths from the Borborema Pegmatite Province, Northeastern Brazil. The Canadian Mineralogist 45(6): 1367-1387.

Černý, P. 1991. Fertile granites of Precambrian rare-element pegmatite fields: is geochemistry controlled by tectonic setting or source lithologies? Precambrian Research 51(1-4): 429-468.

Černý, P. and Chapman, R. 2001. Exsolution and breakdown of scandian and tungstenian Nb–Ta–Ti–Fe–Mn phases in niobian rutile. The Canadian Mineralogist 39(1): 93-101.

Černý, P. and Ercit, T.S. 1989. Mineralogy of niobium and tantalum: crystal chemical relationships, paragenetic aspects and their economic implications. In: Möller, P., Černý, P. and Saupé, F. (eds.), Lanthanides, Tantalum and Niobium. Springer-Verlag: 27-79, Berlin.

Černý, P., Čech, F. and Povondra, P. 1964. Review of ilmenorutile-strüverite minerals. Neues Jahrbuch für Mineralogie - Abhandlungen 101: 142-172.

Černý, P., Chapman, R., Simmons, W.B. and Chackowsky, L.E. 1999. Niobian rutile from the McGuire granitic pegmatite, Park County, Colorado: Solid solution, exsolution, and oxidation. American Mineralogist 84: 754-763.

Černý, P., Ercit, T.S. and Wise, M.A. 1992a. The tantalite – tapiolite-(Fe) gap: natural assemblages versus experimental data. The Canadian Mineralogist 30(3): 587-596.

Černý, P., Novák, M. and Chapman, R. 1992b. Effects of sillimanite-grade metamorphism and shearing on Nb,Ta-oxide minerals in granitic pegmatites: Maršíkov, northern Moravia, Czechoslovakia. The Canadian Mineralogist 30(3): 699-718

Černý, P., Novák, M. and Chapman, R. 2000. Subsolidus behavior of niobian rutile from Věžná, Czech Republic: A model for exsolutions in phases with Fe^{2+}>> Fe^{3+}. Journal of Geosciences 45(1-2): 21-35.

Černý, P., Novák, M., Chapman, R. and Ferreira, K.J. 2007. Subsolidus behavior of niobian rutile from the Písek region, Czech Republic: a model for exsolution in W- and Fe^{2+}>>-Fe^{3+}-rich phases. Journal of Geosciences 52: 143-159.

Černý, P., Pau, I.B.J., Hawthorne, F.C. and Chapman, R. 1981. A niobian-rutile – disordered columbite intergrowth from the Huron Claim pegmatite, southeastern Manitoba. The Canadian Mineralogist 19(4): 541-548.

Chládek, Š., Uher, P. and Novák, M. 2020. Compositional and textural variations of columbite-group minerals from beryl-columbite pegmatites, the Maršíkov District, Bohemian Massif, Czech Republic: magmatic versus hydrothermal evolution. The Canadian Mineralogist 58(6): 767-783.

Chládek, Š., Uher, P., Novák, M., Bačík, P. and Opletal, T. 2021. Microlite-group minerals: tracers of complex post-magmatic evolution in beryl–columbite granitic pegmatites, Maršíkov District, Bohemian Massif, Czech Republic. Mineralogical Magazine 85(5): 725-743.

Christy, A.G. and Atencio, D. 2013. Clarification of status of species in the pyrochlore supergroup. Mineralogical Magazine 77(1): 13-20.

Chukanov, N.V., Pasero, M., Aksenov, S.M., Britvin, S.N., Zubkova, N.V., Yike, L. and Witzke, T. 2023. Columbite supergroup of minerals: nomenclature and classification. Mineralogical Magazine 87(1): 18-33.

Colombo, F. 2008. Polimorfos del TiO2 de aplitas-pegmatitas de Papachacra, Provincia de Catamarca. 9° Congreso de Mineralogìa y Metalogenia, Actas: 1-8. Buenos Aires.

Craig, J.R. and Vaughan, D.J. 1994. Ore microscopy and ore petrography. 2nd edn. John Wiley & Sons, Inc., 434 p., New York.

Fernández, R.R., Schalamuk, I.B.A. and Omenetto, P. 2005. Composición del rutilo como indicador de las condiciones de formación del greisen del distrito Mazán (Sn-W), provincia de La Rioja. Revista de la Asociación Geológica Argentina 60: 259-267.

Galliski, M.Á., Márquez-Zavalía, M.F. Černý, P. and Lira, R. 2016. Complex Nb–Ta–Ti–Sn oxide mineral intergrowths in La Calandria pegmatite, Cañada del Puerto, Córdoba, Argentina. The Canadian Mineralogist 54(4): 899-916.

Galliski, M.Á., Márquez-Zavalía, M.F., Škoda, R., Novák, M., Čopjaková, R. and Pagano, D.S. 2019. A Ta, Ti–rich oxide mineral assemblage from the Nancy beryl–columbite–phosphate granitic pegmatite, San Luis, Argentina. Mineralogy and Petrology 113(5): 687-701.

Geisler, T., Schaltegger, U. and Tomaschek, F. 2007. Re-equilibration of zircon in aqueous fluids and melts. Elements 3(1): 43-50.

Hogarth, D.D. 1977. Classification and nomenclature of the pyrochlore group. American Mineralogist 62(5-6): 403-410.

Hogarth, D.D., and Horne, J.E.T. 1989. Non-metamict uranoan pyrochlore and uranpyrochlore from tuff near Ndale, Fort Portal area, Uganda. Mineralogical Magazine 53(370): 257-262.

Klementová, M. and Rieder, M. 2004. Exsolution in niobian rutile from the pegmatite deposit at Greenbushes, Australia. The Canadian Mineralogist 42(6): 1859-1870.

Laugier, J. and Bochu, B. 2003. CELREF – Programme d'affinement des paramètres de maille à partir d'un diagramme de poudre développé au Laboratoire des Matériaux et du Génie Physique, Ecole Nationale Supérieure de Physique de Grenoble (INPG) Domaine Universitaire

BP 46, 38402, St. Marin d'Hères. http:www.ccp14.ac.uk/tutorial/emgp/celref.htm.

Lira, R., Biglia, M.E., Guereschi, A.B., Bulatovich, S. and Valdez, M.A. 2018. Rutilo del Cordón Centenario, Puna Austral, Salta: mineralogía y origen. Revista de la Asociación Geológica Argentina 75(3): 380-395.

Lira, R., Gay, H-D., Kirschbaum, A.M. and Martínez, E.B. 1987. Minerales pesados de dos facies graníticas del extremo septentrional del batolito de Las Chacras, Sierra de San Luis, Argentina. Academia Nacional de Ciencias, Misceláneas 74: 17.

Lira, R., Galliski, M.A., Bernard, F. and Roquet, M.B. 2012. The intragranitic Potrerillos NYF pegmatites and their A-type host granites of the Las Chacras – Potrerillos batholith, Sierra de San Luis, Argentina. The Canadian Mineralogist 50(6): 1729-1750.

Lumpkin, G.R., Chakoumakos, B.C. and Ewing, R.C. 1986. Mineralogy and radiation effects of microlite from the Harding pegmatite, Taos County, New Mexico. American Mineralogist 71(3-4): 569-588.

Martin, R.F. and De Vito, C. 2014. The late-stage miniflood of Ca in granitic pegmatites: an open-system acid-reflux model involving plagioclase in the exocontact. The Canadian Mineralogist 52(2): 165-181.

Nasdala, L., Kronz, A., Wirth, R., Váczi, T., Perez-Soba, C., Willner, A. and Kennedy, A.K. 2009. The phenomenon of deficient electron microprobe totals in radiation-damaged and altered zircon. Geochimica et Cosmochimica Acta 73(6): 1637-1650.

Novák, M., Johan, Z., Škoda, R., Černý, P., Šrein, V. and Veselovský, F. 2008. Primary oxide minerals in the system WO_3–Nb_2O_5–TiO_2–Fe_2O_3–FeO and their breakdown products from the pegmatite No. 3 at Dolní Bory-Hate, Czech Republic. European Journal of Mineralogy 20(4): 487-499.

Okrusch, M., Hock, R., Schüssler, U., Brummer, A., Baier, M. and Theisinger, H. 2003. Intergrown niobian rutile phases with Sc-and W-rich ferrocolumbite: An electron-microprobe and Rietveld study. American Mineralogist 88(7): 986-995.

Pouchou, J.L. and Pichoir, F. 1985. "PAP" (phi-rho-z) procedure for improved quantitative microanalysis. In Armstrong, J.T. (ed.), Microbeam Analysis. San Francisco Press: (104-106), San Francisco, California.

Rabbia, O.M. and Hernández, L.B. 2012. Mineral chemistry and potential applications of natural- multi-doped hydrothermal rutile from porphyry copper deposits. In: It-Meng (Jim) Low (ed.), Rutile: Properties, Synthesis and Applications: 209-228.

Roquet, M.B. 2010. Mineralogía, Geoquímica, Tipología y Relación con los Granitoides de las Pegmatitas del Grupo Villa Praga – Las Lagunas, Distrito Conlara, Sierra De San Luis. Ph.D. thesis, Universidad Nacional de Córdoba, Argentina (unpublished), 415 p., Córdoba.

Roquet, M.B., Bernard, F., Lira, R. and GallIski, M.A. 2011. The NYF pegmatites of the Potrerillos granite, Sierras de San Luis, Argentina. Revista de la Asociación Geológica Argentina Serie D, Publicación Especial 14: 169-171.

Zachař, A., Novák, M. and Škoda, R. 2020. Beryllium minerals as monitors of geochemical evolution from magmatic to hydrothermal stage; examples from NYF pegmatites of the Třebíč Pluton, Czech Republic. Journal of Geosciences 65(3): 153-172.

Zaitsev, A.N., Spratt, J., Shtukenberg, A.G., Zolotarev, A.A., Britvin, S.N., Petrov, S.V., Kuptsova, A.V. and Antonov, A.V. 2021. Oscillatory-and sector-zoned pyrochlore from carbonatites of the Kerimasi volcano, Gregory rift, Tanzania. Mineralogical Magazine 85(4): 532-553.